Handling Gaussian blur without deconvolution

Jitka Kostková [a], Jan Flusser [a,*], Matěj Lébl [a], Matteo Pedone [b]

[a] *Czech Academy of Sciences, Institute of Information Theory and Automation, Pod vodárenskou věží 4, 182 08 Prague 8, Czech Republic*
[b] *Center for Machine Vision Research, Department of Computer Science and Engineering, University of Oulu, Oulu FI-90014, Finland*

ARTICLE INFO

ABSTRACT

The paper presents a new theory of invariants to Gaussian blur. Unlike earlier methods, the blur kernel may be arbitrary oriented, scaled and elongated. Such blurring is a semi-group action in the image space, where the orbits are classes of blur-equivalent images. We propose a non-linear projection operator which extracts blur-insensitive component of the image. The invariants are then formally defined as moments of this component but can be computed directly from the blurred image without an explicit construction of the projections. Image description by the new invariants does not require any prior knowledge of the blur kernel parameters and does not include any deconvolution. The invariance property could be extended also to linear transformation of the image coordinates and combined affine-blur invariants can be constructed. Experimental comparison to three other blur-invariant methods is given. Potential applications of the new invariants are in blur/position invariant image recognition and in robust template matching.

1. Introduction

In image processing and analysis, we often have to deal with images which are degraded versions of the original scene. One of the most common degradations is *blur*, which usually appears as a smoothing or suppression of high-frequency details of the image. Capturing an ideal scene *f* by an imaging device with the point-spread function (PSF) *h*, the observed image *g* can be modeled as a convolution of both

$$g(\mathbf{x}) = (f * h)(\mathbf{x}). \tag{1}$$

This linear image formation model, even if it is very simple, is a reasonably accurate approximation of many imaging devices and acquisition scenarios. In this paper, we concentrate our attention to the case when the PSF is a Gaussian function with unknown parameters.

Gaussian blur appears whenever the image has been acquired through a turbulent medium and the acquisition/exposure time is by far longer than the period of Brownian motion of the particles in the medium. Random fluctuations of the refractive index perturb the phase of the light and blur the acquired image. Ground-based astronomical imaging through the atmosphere, long-distance aerial and satellite surveillance, taking pictures through a haze, un-

derwater imaging, and fluorescence microscopy are typical examples of such situation (in some cases, the blur may be coupled with a contrast decrease). Gaussian blur is also introduced into the images as the sensor blur which is due to a finite size of the sampling pulse. It may be sometimes applied intentionally as a low-pass filter for noise suppression, as a graphic tool to soften the image, and as a preprocessing when building the scale-space image pyramid to prevent aliasing artifacts. Few examples of Gaussian-blurred images can be seen in Fig. 1.

Eq. (1) is an example of an *inverse problem*, where we want to estimate *f* from its degraded version *g*, while the PSF may be partially known or unknown. This task is ill posed. Without additional constraints, infinitely many solutions satisfying Eq. (1) may exist. Solving of (1) has been known in image processing literature as *image restoration* and can be traced back to 1960's. Despite of its long history, it has not been fully resolved. Although some of the current image restoration and deconvolution methods yield good results, they rely on prior knowledge incorporated into regularization terms or in other constraints. If such prior knowledge is not available, the methods may diverge or converge to a solution which is far from the ground truth. In case of a Gaussian blur, the parametric shape of the PSF can be used as a prior but another specific problem appears. Since any Gaussian function is infinitely divisible (it can be expressed as a convolution of arbitrary number of Gaussians) and since the convolution is an associative operation, the deconvolution may eliminate only a part of the actual blur, while the rest of the blur may be mistakenly considered as a part of the

* Corresponding author.
E-mail addresses: kostkova@utia.cas.cz (J. Kostková), flusser@utia.cas.cz (J. Flusser), lebl@utia.cas.cz (M. Lébl), matped@ee.oulu.fi (M. Pedone).
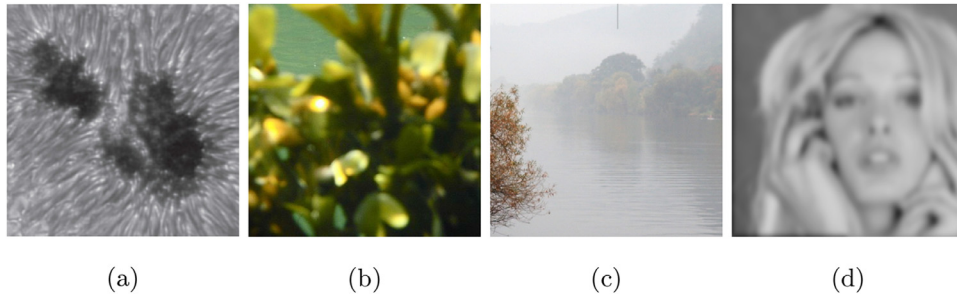
Fig. 1. Examples of the Gaussian blur: (a) a sunspot blurred by atmospheric turbulence, (b) underwater photo blurred by light dispersion, (c) a picture taken through haze, (d) a digitally low-pass filtered image.
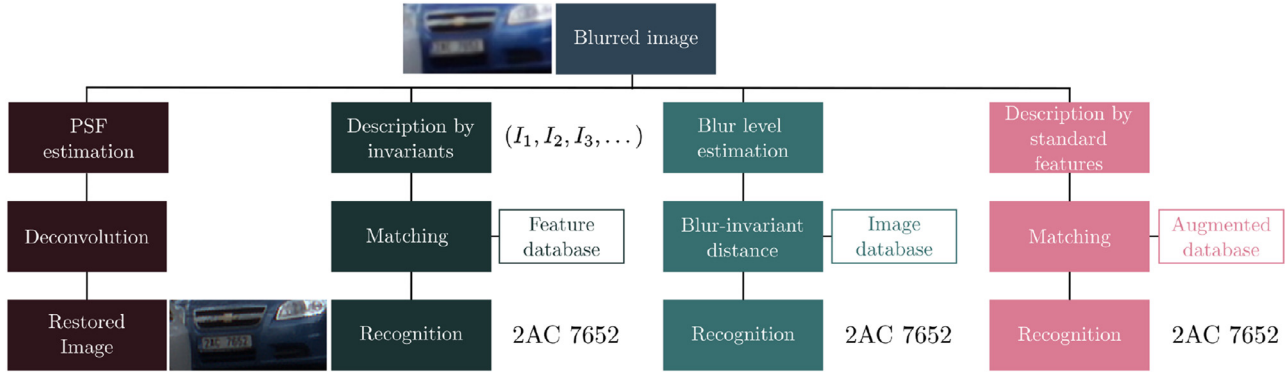

Fig. 2. Four approaches to analysis of blurred images. Image restoration via deconvolution (first branch), description and recognition by blur invariants (second branch), matching by minimum blur-invariant distance (third branch), and brute-force searching an augmented database (last branch).

original image. From a purely mathematical point of view, there is in principle no chance to avoid these formally correct but actually false solutions if no other prior information is available.

In 1990's, some researchers not only realized all the above-mentioned difficulties connected with the solving of Eq. (1) but also found out that in many applications a complete restoration of f is not necessary and can be avoided, provided that an appropriate image representation is used. A typical example is a recognition of objects in blurred images, where a blur-robust object description forms a sufficient input for the classifier. This led to introducing the idea of *blur invariants*. Roughly speaking, blur invariant I is a functional fulfilling the constraint $I(f) = I(f * h)$ for any h from a certain set S of admissible PSF's. Many systems of blur invariants have been proposed so far. They differ from one another by the assumptions on the PSF, by the mathematical tools used for invariant construction, by the domain in which the invariants are defined, and by the application area which the invariants were designed for (see [1], Chapter 6, for a survey of blur invariants and further references).

Instead of constructing blur invariants of an individual image, in a few papers the authors proposed rather to use *blur-invariant distance* to measure the similarity between a blurred query image and clear database elements. This may help for such PSF's for which the invariants $I(f)$ are difficult to design or expensive to calculate.

The last group of methods replaces the theoretical construction of blur invariants with a brute-force search of an augmented database, which contains numerous samples of artificially generated blurred versions of each clear database image.

Fig. 2 illustrates the differences between these four approaches. Relevant work of all these categories are reviewed in Section 2.

All current methods dealing with Gaussian blur, regardless of the category they belong to, suffer from two serious limitations. The first one is that they were designed for *circular* Gaussian blur only and cannot handle more general scenarios. The assumption of the circular symmetry of the blur is an intrinsic aspect of most methods. The generalization from circular to anisotropic arbitrary oriented Gaussian blur is non-trivial and requires completely new approaches. The second limitation, which is partially connected with the first one, is that almost all current methods cannot handle simultaneously the blur and geometric transformations, such as rotation, scaling and affine transformation. They either cannot be adapted to handle spatial transformations at all (this is true namely for the invariant distances) or the possibility of the adaptation is coupled with the assumption of circular blur, which must not be violated under the spatial transformation (which is not the case of an affine transform). Since in practical applications the template rotation/scaling/affine transform may be present quite often, this is a serious drawback. One might think that an anisotropic Gaussian blur does not appear often in practice but the opposite is true. If the sensor has different resolution in horizontal and vertical direction then, even if the ground-truth PSF is circular, the image is blurred differently in x and y. If, moreover, the sensor parameters are not adjusted w.r.t. the database images, we face the problem of recognition of rotated/scaled/skewed and blurred images by an arbitrary-shaped Gaussian. An anisotropic Gaussian blur appears also if the turbulence in the medium, we are taking the picture through, is in certain direction more significant (due to wind for instance) than in the others. All this is a clear call for a discovery of more advanced invariants.

The main novel contribution of this paper is the design of the *combined invariants* to Gaussian blur and spatial affine transformation. This problem has not been tackled in the literature so far. This is accomplished through a derivation of the invariants w.r.t. blurring with a general (anisotropic) Gaussian kernel. The new blur invariants are defined by means of non-linear projection operators and are able to handle much more general scenarios than any other existing method, as we demonstrate by experiments. This brings immediate practical benefits. When applying the earlier

invariants, we should first check whether or not the Gaussian blurring PSF is circularly symmetric, which is almost impossible to verify from the blurred image itself. If this constraint has not been met, the method fails. The new invariants presented in this paper can be applied directly and do not require any prior estimation of the blurring PSF. The proposed combination with a rotation/affine invariance is based on the *Substitution Theorem*, which crowns the paper.

The paper is structured as follows. After the literature survey given in the next Section, we introduce the mathematical background of Gaussian blur in Section 3. Blur invariants in Fourier domain are proposed in Section 4 and their counterparts in image domain, moment-based blur invariants, are presented in Section 5. In Section 6, we formulate the Substitution Theorem, which allows to construct combined blur-affine invariants. Section 7 presents several recognition experiments on real real images and video.

2. Related work

State-of-the-art methods, dealing with the model (1) and with Gaussian blur, can be categorized into four main groups. In the sequel, we give a brief overview of each of them.

2.1. Restoration methods

Several image restoration methods specifically designed for Gaussian blur have been published. They try to estimate the size (variance) of the blur and perform a non-blind deconvolution. Honarvar et al. [2] proposed to perform the deconvolution in the moment domain but that algorithm contains a time-consuming search in the parametric space and is sensitive to overestimation of the Gaussian variance. The APEX method [3] estimated the blur variance by fitting the image spectrum in the Fourier domain. There exist also several local methods that estimate the blur size by investigating the response on a point source or on an ideal edge [4,5]. A common weakness of these methods is their sensitivity to noise and the necessity of the prior knowledge where an ideal point or edge is located. Xue and Blu [6] proposed to estimate the blur variance by minimizing a proper functional and then to apply a non-blind Wiener filtering. As in the previous cases, the method is sensitive to the variance overestimation and relatively time consuming. Numerous other methods were developed specially for atmospheric turbulence restoration [7] and most of the general blind-deconvolution algorithms (see, for instance, [8] for a survey and further references) can be used for Gaussian blur restoration as well with average results.

Restoration methods are not direct competitors of the proposed invariant-based technique. They were primarily designed to yield an estimation of the ideal image for visual interpretation. When used for recognition purposes, they serve as a pre-processing of the query image which is then described by some standard features. Such approach is, however, slow and unstable due to the restoration artifacts.

2.2. Brute force and convolution neural networks

A brute-force approach to recognition of degraded images relies on high computational power of current super-computers. To avoid both inversion of the degradation model as well as the design of the invariants, the training set is extended with all assumable degradations (using a proper sampling of the parametric space) of the training images. This process is called *data augmentation* and is popular especially in the connection with deep convolution neural networks (CNNs) where it may improve the recognition rate, see for instance [9]. Large-scale data augmentation is, however, time and memory consuming. In our case, the augmentation would require to generate blurred and spatially deformed versions of each training image with Gaussian kernels and transformation parameters from a certain range, and a consequent massive training. Since this would enlarge the training set by several orders, it is clear that this is not a feasible solution for databases containing many classes. Without data augmentation, even the state-of-the-art CNNs that perform excellently on clear images fail frequently when recognizing blurred inputs. As shown experimentally in [10], their performance drops when they are used to recognize degraded images while they have been trained on clear images only [10].

2.3. Blur-invariant distances

The idea of blur-invariant distance was firstly proposed by Zhang et al. [11] and has found several successors. All algorithms of this kind try to define a distance between two images, which fulfills the constrain $d(f_1, f_2) = d(f_1 * h, f_2)$ for any admissible h.

Zhang et al. [11,12] assumed circular Gaussian blur, estimated the blur level of the images to be compared (the authors took the integral of the image Laplacian as the blur estimator) and brought the images to the same blur level by blurring of the one which was less blurred. The distance $d(f_1, f_2)$ is then defined either as a weighted L_2-distance between the images of the same blur level [11] or as a geodesic distance on the surface of the manifold which contains the images of the same blur level [12]. The advantage of the Zhang's method is its simplicity. It does not contain any deblurring, minimization and iterations. However, the proposed estimation of the blur level is questionable for two images with different amount of high-frequency information.

Gopalan et al. [13] derived another blur-invariant distance measure without assuming the knowledge of the blur shape but they imposed a limitation on the blur support size. The authors showed that all blurred versions of the given image create a linear subspace, which can be understood as a point on Grassmann manifold. The blur-invariant distance between two images is then defined as the Riemannian distance between two points on the manifold. At the same time, this can be equivalently understood as measuring the angle between two subspaces. Although the Gopalan's method does not explicitly use the parametric shape of the blur, it performs well on Gaussian blur. However, the method suffers from two major drawbacks – the absence of any constraints imposed on the blur (except the support size) admits physically non-realistic blurs with negative values and the calculation of the Riemannian distance is very time-consuming.

The Gopalan's method was improved by Vageeswaran et al. [14], who introduced the positivity and energy-preserving constraints into the Gopalan's method. Under these constraints, blur-equivalent images form a convex set in the image space. The blur-invariant distance between the query image and the template is defined as the distance between the point, representing the query image, and its projection onto the convex set containing all blurred versions of the template. Most recently, essentially the same idea was independently proposed by Lébl et al. [15] who also presented an efficient algorithm for distance calculation by quadratic programming.

Fig. 3 visualizes, in a simplified way, the differences between the above mentioned distance measures. All three measures are compared to the proposed method in the experiments in Section 7.

2.4. Explicit blur invariants

Invariants w.r.t. blur were originally proposed in the work by Flusser et al. [16,17]. The first blur invariants were invariant w.r.t. any centrosymmetric PSF, without taking into account its parametric form. In 2015, Flusser et al. proposed a general theory of linear
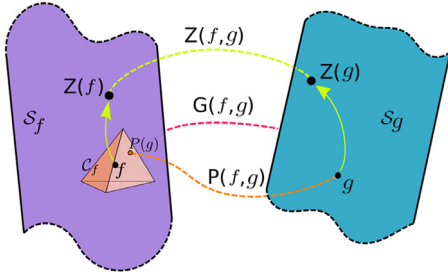
Fig. 3. Illustration of three blur invariant distances: Zhang's (Z) "image to image", Gopalan's (G) "subspace to subspace" and Lébl's and Vageeswaran's (P) "image to a convex set".

Fig. 4. 2D general Gaussian function with the principal eigenvector oriented in approx 30 degrees and with the eigenvalue ratio 6.

projection operators [18], which allowed to design specific blur invariants w.r.t. arbitrary *N*-fold symmetric blur, which led to an increase of their discriminability. The literature on blur invariants is relatively rich. Below we review only those methods, that were designed specifically for Gaussian blur. If a parametric Gaussian form of the blur kernel is assumed, the general invariants from [18] and similar can be still used but do not provide the optimal discrimination power.

Liu and Zhang [19] realized that the complex moments of the image, one index of which is zero, are invariant to Gaussian blur. Xiao [20] seemingly derived invariants to Gaussian blur but in fact he only employed the symmetry of the Gaussian rather than its parametric form. Höschl proposed invariants to Gaussian convolution in 1D and applied them to image histograms [21]. Flusser et al. [22] introduced a complete set of moment-based Gaussian blur invariants for the case that the Gaussian PSF is circularly symmetric. The experimental evaluation in [22] shows that these invariants, thanks to their specificity, outperform in template-matching experiments general methods such as cross-correlation, local phase quantization (LPQ) [23] and centrosymmetric blur invariants [17]. They even performed better than the Zhang's distance [12].

Serious weakness of all above mentioned Gaussian-blur invariant methods is that they assume circularly symmetric Gaussian blur only. Some of them, such as [12] and [22], could be generalized to work with elongated Gaussian blur in axial position (i.e. with a diagonal covariance matrix) but it is not possible to go beyond this limitation. This is also the reason why these methods cannot combine the invariance to blur with the invariance to image rotation and/or affine transformation, which is a critical limitation for practical usage.

Most recently, Kostková et al. [24] published the first paper ever on invariants w.r.t. Gaussian blur with a non-diagonal covariance matrix. In this paper, we adopt some preliminary results published in [24]. However, the idea of the combined invariants was not mentioned in [24].

3. Gaussian blur

In this section, we establish the necessary mathematical background which will be later used for designing the invariants.

By *d*-dimensional *image function* (or just image for short) $f(\mathbf{x})$ we understand any function from $L_1(\mathbb{R}^d)$, the integral of which is nonzero. For the sake of generality, we do not constrain it to be non-negative. In this paper, we are mostly dealing with 2D images, but many conclusions are valid or can be readily extended to arbitrary *d*.

By *d*-dimensional Gaussian G_Σ we understand the function

$$G_\Sigma(\mathbf{x}) = \frac{1}{(2\pi)^{d/2}\sqrt{|\Sigma|}} \exp\left(-\frac{1}{2}\mathbf{x}^T\Sigma^{-1}\mathbf{x}\right), \tag{2}$$

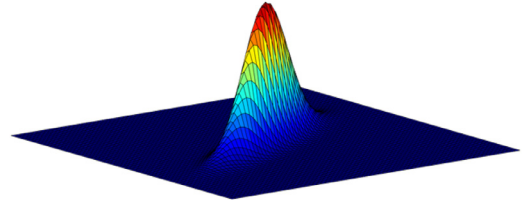where $\mathbf{x} \equiv (x_1, x_2, \ldots, x_d)^T$ and Σ is a $d \times d$ regular covariance matrix. Since the covariance matrix is positive definite, we have, for its determinant, $|\Sigma| > 0$. We consider centralized Gaussians only (convolution with a non-centralized PSF just introduces an extra shift of the image).

The covariance matrix determines the shape of the Gaussian. If it is a multiple of a unitary matrix, then we get a circularly symmetric function. If it is diagonal but not unitary, we obtain an "elongated" Gaussian with elliptical contours in the axial position (in that case, *d*-dimensional Gaussian can be factorized into a product of *d* one-dimensional Gaussians). Generally, the Gaussian may be arbitrary oriented and elongated. The eigenvectors of Σ define the axes of the Gaussian and the eigenvalues determine its elongation (see Fig. 4).

The set *S* of all Gaussian blurring kernels is

$$S = \{aG_\Sigma | a > 0, \Sigma \ \text{positive definite}\}. \tag{3}$$

Note that *S* is not a linear vector space because the sum of two different Gaussians is not a Gaussian. For the sake of generality, we consider un-normalized kernels to be able to model also a change of the image contrast. The basic properties of the set *S* are listed below. The *closure properties* play the most important role in deriving invariants.

Proposition 1 (Integrability). *$S \subset L_1$ since $\int aG_\Sigma = a$.*

Proposition 2 (Convolution closure). *S is closed under convolution as*

$$a_1G_{\Sigma_1} * a_2G_{\Sigma_2} = a_1a_2G_{\Sigma_1+\Sigma_2}.$$

Proposition 3 (Multiplication closure). *S is closed under point-wise multiplication as*

$$a_1G_{\Sigma_1} \cdot a_2G_{\Sigma_2} = aG_\Sigma,$$

where

$$a = \frac{a_1a_2}{(2\pi)^{d/2}\sqrt{|\Sigma_1 + \Sigma_2|}}$$

and $\Sigma = \left(\Sigma_1^{-1} + \Sigma_2^{-1}\right)^{-1}$.

Proposition 4 (Fourier transform closure). *Fourier transform of a function from S always exists, lies in S and is given by*

$$\mathcal{F}(aG_\Sigma) = \frac{a}{(2\pi)^{d/2}\sqrt{|\Sigma|}}G_{\Sigma_1},$$

where

$$\Sigma_1 = \frac{1}{4\pi^2}\Sigma^{-1}.$$

Proposition 5 (Coordinate transform closure). *Let A be a regular $d \times d$ matrix describing a linear transform of the coordinates. Then S turns to itself under the transform $\mathbf{x}' = A\mathbf{x}$. This follows from the fact that*

$$aG_\Sigma(A\mathbf{x}) = \frac{a}{\|A\|}G_{A^{-1}\Sigma A^{-T}}(\mathbf{x}),$$

where $\|A\|$ means the absolute value of the determinant of A and $A^{-T} \equiv (A^T)^{-1} = (A^{-1})^T$.

In the sequel, we use a slightly extended definition of S with Dirac δ-function being incorporated

$$S = \{aG_\Sigma | a > 0, \Sigma \text{ positive definite}\} \cup \{a\delta\}. \tag{4}$$

Proposition 2, along with the associativity of convolution, says that $(S, *)$ is a *semi-group* (it is not a group since convolution is not invertible within S). Hence, convolution with a function from S is a *semi-group action* on L_1.

The image space L_1 is factorized into *blur-equivalent classes* by the following relation. We say that the images f and g are Gaussian blur equivalent ($f \sim g$), if and only if there exist $h_1, h_2 \in S$ such that $h_1 * f = h_2 * g$. Thanks to Proposition 2 and to the commutativity of convolution, this relation is transitive, while symmetry and reflexivity are obvious. At the same time, the equivalence classes of $L_1/_\sim$ are related to the *orbits* of the above mentioned semi-group action. An orbit, originating from image f, is the set of all images that can be obtained from f as the result of the semi-group action. We will later show that the classes of $L_1/_\sim$ are exactly the same as the orbits generated by certain special images (this assertion will be formulated as Theorem 2 in Section 4).

The main idea of this paper is the following. We are going to find these "origins" of the orbits (we will call them *primordial images*) and describe them by means of properly chosen descriptors – *invariants* of the orbits. For instance, the set S itself forms an orbit with δ being its primordial image. The invariants stay constant within each equivalence class, while should distinguish any two images belonging to different classes. The invariance in question is in fact the invariance w.r.t. arbitrary Gaussian blur. The main trick, which makes this theory practically applicable, is that the invariants can be calculated from the given blurred image without explicitly constructing the primordial image.

In Section 4, we define a *projection operator* that "projects" each image onto S. The primordial images and, consequently, Gaussian blur invariants are constructed by means of this projection operator.

4. Projection operators and blur invariants

In linear algebra, projection operators onto linear subspaces are a well-established tool to decompose the given space into a direct sum of two subspaces, which usually have distinct properties. The idea of projecting the image space onto proper subspaces and then to define the image invariants in one of them was originally proposed by Flusser et al. in [18], where the invariants w.r.t. convolution with a symmetric non-parametric kernel were proposed. The authors constructed the projection onto the kernel subspace and defined the invariants in the complementary subspace.

In this paper, we face an analogous situation – we may try to construct the image projection onto the set S, eliminate somehow this Gaussian component of the image and define the invariants in the complement. However, there is a significant difference from the mathematical point of view. While in [18], linear projections onto linear, mutually orthogonal, subspaces were sufficient to resolve the problem, here we have to find a projection onto the set S of Gaussian kernels, which is not a linear subspace. Clearly, the respective projection operator cannot be linear and must be constructed in a different way than the operators proposed in [18].

Let us define the projection operator P such that it projects an image f onto the nearest un-normalized Gaussian, where the term "nearest" means the Gaussian having the same integral and covariance matrix as the image f itself. So, for $d = 2$ we define

$$Pf = m_{00}G_C, \tag{5}$$

where

$$C = \frac{1}{m_{00}} \begin{pmatrix} m_{20} & m_{11} \\ m_{11} & m_{02} \end{pmatrix},$$

and m_{pq} is the centralized image moment

$$m_{pq} = \int \int (x - c_1)^p (y - c_2)^q f(x, y) \, dx \, dy \tag{6}$$

with (c_1, c_2) being the image centroid.

Clearly, P is well defined for all "common" images[1] and actually if Pf exists, then always $Pf \in S$. Although P is not linear, it can still be called projection operator, because it is idempotent, i.e. $P^2 = P$. In particular, $P(aG_\Sigma) = aG_\Sigma$. Pf can be understood as a Gaussian component of f. Note, that the Gaussian component depends both on the image content and on the Gaussian blur (if any). Both factors contribute jointly to Pf. So, Pf is not an estimate of the actual blur kernel.

The key property of P, which will be later used for construction of the invariants, is that it commutes with a convolution with a Gaussian kernel, as shown in the following lemma.

Lemma 1. *Let P be the above-defined projector, $f \in L_1$ be an image function such that Pf exists and let $G_\Sigma \in S$. Then it holds*

$$P(f * G_\Sigma) = Pf * G_\Sigma. \tag{7}$$

Proof. To prove this lemma, we first recall how the image central moments are transformed under convolution. For arbitrary f and h we have

$$m_{00}^{(f*h)} = m_{00}^{(f)} m_{00}^{(h)},$$
$$m_{20}^{(f*h)} = m_{20}^{(f)} m_{00}^{(h)} + m_{00}^{(f)} m_{20}^{(h)},$$
$$m_{11}^{(f*h)} = m_{11}^{(f)} m_{00}^{(h)} + m_{00}^{(f)} m_{11}^{(h)},$$
$$m_{02}^{(f*h)} = m_{02}^{(f)} m_{00}^{(h)} + m_{00}^{(f)} m_{02}^{(h)}.$$

Considering the projection of $f * G_\Sigma$, it must have a form $P(f * G_\Sigma) = aG_K$, where $a = m_{00}^{(f*G_\Sigma)} = m_{00}^{(f)}$ and

$$K = \frac{1}{m_{00}} \begin{pmatrix} m_{20} + m_{00}\Sigma_{20} & m_{11} + m_{00}\Sigma_{11} \\ m_{11} + m_{00}\Sigma_{11} & m_{02} + m_{00}\Sigma_{02} \end{pmatrix}.$$

All moments m_{pq} in the above equation are related to f. Hence, $K = C + \Sigma$. On the other hand, we have

$$Pf * G_\Sigma = m_{00}G_C * G_\Sigma = m_{00}G_{C+\Sigma}.$$

The last equality follows from Proposition 2. □

Now we can formulate the Fundamental theorem on blur invariants.

Theorem 1. *Let P be the above-defined projector and let f be an image function such that Pf exists. Then*

$$I(f) = \frac{\mathcal{F}(f)}{\mathcal{F}(Pf)} \tag{8}$$

is an invariant to Gaussian blur, i.e. $I(f) = I(f * h)$ for any $h \in S$.

Proof. The proof follows immediately from Lemma 1.

$$I(f * h) = \frac{\mathcal{F}(f * h)}{\mathcal{F}(P(f * h))} = \frac{\mathcal{F}(f)\mathcal{F}(h)}{\mathcal{F}(Pf * h)} = \frac{\mathcal{F}(f)\mathcal{F}(h)}{\mathcal{F}(Pf)\mathcal{F}(h)} = \frac{\mathcal{F}(f)}{\mathcal{F}(Pf)} = I(f)$$

□

Note that if Pf exists, then $I(f)$ is well defined on all frequencies because the denominator $\mathcal{F}(Pf)$ is a Gaussian and hence non-zero everywhere.

---

[1] If $m_{00} = 0$ or if C is not positive definite or if some second-order moment(s) are infinite, then Pf is undefined. Although such functions exist in L_1, they do not describe real-life images and we do not consider them in this paper.
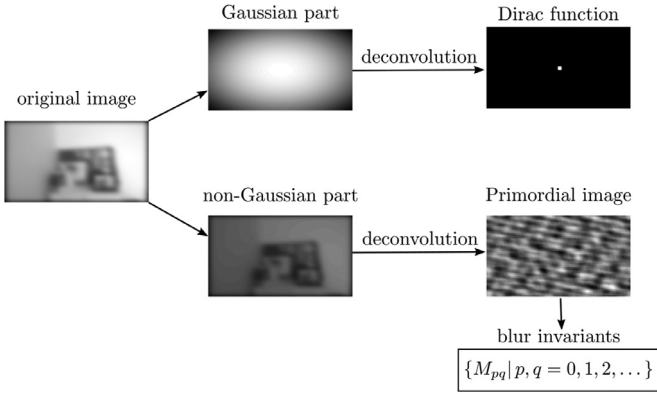
Fig. 5. Visualization of the main idea: The image is projected onto a set of Gaussians and this projection (i.e. the Gaussian part of the image) is used to "deconvolve" the image in Fourier domain. Blur-invariant primordial image is obtained as the result of this operation. Moments of the primordial image are blur invariants introduced in Eq. (15).

The following Theorem says that the invariant $I(f)$ is *complete*, which means the equality $I(f_1) = I(f_2)$ occurs if and only if f_1 and f_2 belong to the same equivalence class.

Theorem 2. *Let f_1 and f_2 be two image functions and $I(f)$ be the invariant defined in Theorem 1. Then $I(f_1) = I(f_2)$ if and only if there exist h_1, $h_2 \in S$ such that $h_1 * f_1 = h_2 * f_2$.*

The proof is straightforward by setting $h_1 = Pf_2$ and $h_2 = Pf_1$. The completeness guarantees that $I(f)$ discriminates between the images from different equivalence classes, while stays constant inside each class due to the invariance property. This assertion not only shows the limitations (the images belonging to the same equivalence class can never be discriminated) but also explains why these invariants outperform general blur invariants if Gaussian blur is present (equivalence classes w.r.t. a general blur are larger than those w.r.t. Gaussian blur).

Invariant $I(f)$ is a ratio of two Fourier transforms which may be interpreted as a deconvolution in frequency domain. Having an image f, we seemingly "deconvolve" it by the kernel Pf. This deconvolution always sends the Gaussian component of f to δ-function. We call the result of this seeming deconvolution the *primordial image*

$$f_r = \mathcal{F}^{-1}(I(f)) .$$

Hence, $I(f)$ can be viewed as Fourier transform of f_r. Note that f_r is actually the "maximally possible" deconvolved image f, which creates the origin of the respective orbit (see Fig. 5 for schematic illustration). Primordial image can be also understood as a kind of normalization (or canonical form) of f w.r.t. arbitrary Gaussian blurring.

It should be noted, that the primordial image is a useful theoretical concept of blur invariants but it is not actually constructed in the implementation of the method. It may lie outside L_1 or may even not exist but it does not matter – the existence of its Fourier transform, the invariants are obtained from, is guaranteed.

5. Invariants in the image domain

Although $I(f)$ itself could serve as an image descriptor, its direct usage brings certain difficulties and disadvantages. On high frequencies, we divide by small numbers which may lead to precision loss. This effect is even more severe if f is noisy. This problem could be overcome by suppressing high frequencies by a low-pass filter, but such a procedure would introduce a user-defined parameter (the cut-off frequency) which should be set up with respect to the particular noise level. Another disadvantage is that we

would have to actually construct $\mathcal{F}(Pf)$ in order to calculate $I(f)$. That is why we prefer to work directly in the image domain, where moment-based invariants equivalent to $I(f)$ can be constructed and evaluated without an explicit calculation of Pf.

First of all, we recall that geometric moments of an image are Taylor coefficients (up to a constant factor) of its Fourier transform[2]

$$\mathcal{F}(f)(\mathbf{u}) = \sum_{\mathbf{p} \geq 0} \frac{(-2\pi i)^{|\mathbf{p}|}}{\mathbf{p}!} m_{\mathbf{p}}^{(f)} \mathbf{u}^{\mathbf{p}} \tag{9}$$

(for simplicity, and also to show the independence of the dimension d, we use the multi-index notation).

Theorem 1 can be rewritten as

$$\mathcal{F}(Pf)(\mathbf{u}) \cdot I(f)(\mathbf{u}) = \mathcal{F}(f)(\mathbf{u}) .$$

All these three Fourier transforms can be expanded similarly to (9) into absolutely convergent Taylor series

$$\sum_{\mathbf{p} \geq 0} \frac{(-2\pi i)^{|\mathbf{p}|}}{\mathbf{p}!} m_{\mathbf{p}}^{(Pf)} \mathbf{u}^{\mathbf{p}} \cdot \sum_{\mathbf{p} \geq 0} \frac{(-2\pi i)^{|\mathbf{p}|}}{\mathbf{p}!} M_{\mathbf{p}} \mathbf{u}^{\mathbf{p}} = \sum_{\mathbf{p} \geq 0} \frac{(-2\pi i)^{|\mathbf{p}|}}{\mathbf{p}!} m_{\mathbf{p}}^{(f)} \mathbf{u}^{\mathbf{p}} , \tag{10}$$

where by $M_{\mathbf{p}}$ we denote the Taylor coefficient of $I(f)$ (we will show later that $M_{\mathbf{p}}$ is in fact the moment of the primordial image).

Comparing the coefficients of the same powers of $\mathbf{u}$ we obtain, for any $\mathbf{p}$,

$$\sum_{\mathbf{k} \leq \mathbf{p}} \frac{(-2\pi i)^{|\mathbf{k}|}}{\mathbf{k}!} \frac{(-2\pi i)^{|\mathbf{p}-\mathbf{k}|}}{(\mathbf{p}-\mathbf{k})!} m_{\mathbf{k}}^{(Pf)} M_{\mathbf{p}-\mathbf{k}} = \frac{(-2\pi i)^{|\mathbf{p}|}}{\mathbf{p}!} m_{\mathbf{p}}^{(f)}, \tag{11}$$

which can be read as

$$\sum_{\mathbf{k} \leq \mathbf{p}} \binom{\mathbf{p}}{\mathbf{k}} m_{\mathbf{k}}^{(Pf)} M_{\mathbf{p}-\mathbf{k}} = m_{\mathbf{p}}^{(f)} . \tag{12}$$

In 2D, Eq. (12) reads as

$$\sum_{m=0}^{p} \sum_{n=0}^{q} \binom{p}{m} \binom{q}{n} m_{mn}^{(Pf)} M_{p-m,q-n} = m_{pq}^{(f)} . \tag{13}$$

Since $Pf = m_{00}^{(f)} G_C$, where C is given by the second-order moments of f, we can express its moments $m_{mn}^{(Pf)}$ without actually constructing the projection Pf. Clearly, $m_{mn}^{(Pf)} = 0$ for any odd $m + n$ due to the centrosymmetry of G_C. For any even $m + n$, $m_{mn}^{(Pf)}$ can be expressed in terms of the moments of f as

$$m_{mn}^{(Pf)} = m_{00}^{(f)} m_{mn}^{(G_C)}$$

$$= m_{00}^{(f)} \sum_{\substack{i=0 \\ j \geq \frac{n-m}{2}}}^{\lfloor \frac{m}{2} \rfloor} \sum_{j=0}^{i} (-1)^{i-j} \binom{m}{2i} \binom{i}{j} (m+n-2i-1)!! \cdot$$

$$\cdot (2i-1)!! \left(\frac{m_{11}}{m_{00}}\right)^{m-2j} \left(\frac{m_{20}}{m_{00}}\right)^{j} \left(\frac{m_{02}}{m_{00}}\right)^{\frac{n-m}{2}+j} . \tag{14}$$

The above expression was obtained by substituting our particular C into the formula for moments of a 2D Gaussian. (The moment formula for a diagonal covariance matrix is well known. For a general covariance matrix, it is not commonly cited in the literature. It can be either deduced from the papers presenting general approaches to moment calculation [25,26] or obtained directly from the definition by integration.)

---

[2] We assume that all moments are finite, which is guaranteed for all images with bounded support.

Now we can isolate M_{pq} on the left-hand side and obtain the recurrence

$$M_{pq} = \frac{m_{pq}^{(f)}}{m_{00}} - \sum_{\substack{l=0 \\ l+k \neq 0, \\ l+k \text{ even}}}^{p} \sum_{k=0}^{q} \binom{p}{l}\binom{q}{k} \sum_{i=0}^{\lfloor \frac{k}{2} \rfloor} \sum_{\substack{j=0 \\ j \geq \frac{k-l}{2}}}^{i} (-1)^{i-j}\binom{k}{2i}\binom{i}{j}(l+k-2i-1)!! \cdot$$

$$\cdot (2i-1)!!\left(\frac{m_{11}}{m_{00}}\right)^{k-2j}\left(\frac{m_{20}}{m_{00}}\right)^{\frac{l-k}{2}+j}\left(\frac{m_{02}}{m_{00}}\right)^{j} M_{p-l,q-k}. \tag{15}$$

This recurrence formula defines Gaussian blur invariants in the image domain. Since $I(f)$ has been proven to be invariant to Gaussian blur, all coefficients M_{pq} must also be blur invariants. The M_{pq}'s can be understood as the moments of the primordial image f_r. The power of Eq. (15) lies in the fact that we can calculate them directly from the moments of f, without constructing the primordial image explicitly either in frequency or in the spatial domain and also without any prior knowledge of the blurring kernel orientation. Thanks to the uniqueness of Fourier transform, the set of all M_{pq}'s carries the same information about the function f as $I(f)$ itself, so the cumulative discrimination power of all M_{pq}'s equals to that of $I(f)$.

Some of the invariants (15) are always trivial. Regardless of f, we have $M_{00} = 1$, $M_{10} = M_{01} = 0$ because we work in centralized coordinates, and $M_{20} = M_{11} = M_{02} = 0$ since these three moments were already used for the definition of Pf. Note that the joint null-space of all M_{pq}'s except M_{00} equals the set S, which is implied by the fact that $P(aG_\Sigma) = aG_\Sigma$ and the corresponding primordial image $f_r^{(S)} = \delta$.

Eq. (15) can be turned to an equivalent non-recursive form

$$M_{pq} = \frac{1}{m_{00}}\sum_{\substack{l=0 \\ l+k \text{ even}}}^{p}\sum_{k=0}^{q}(-1)^{\frac{k+l}{2}}\binom{p}{l}\binom{q}{k}\sum_{i=0}^{\lfloor\frac{k}{2}\rfloor}\sum_{\substack{j=0 \\ j\geq\frac{k-l}{2}}}^{i}(-1)^{i-j}\binom{k}{2i}\binom{i}{j}(l+k-2i-1)!!\cdot$$

$$\cdot (2i-1)!!\left(\frac{m_{11}}{m_{00}}\right)^{k-2j}\left(\frac{m_{20}}{m_{00}}\right)^{\frac{l-k}{2}+j}\left(\frac{m_{02}}{m_{00}}\right)^{j} m_{p-l,q-k}^{(f)}. \tag{16}$$

While the recursive formula is efficient if we want to calculate all invariants up to a certain order, the non-recursive one is useful for calculating a single invariant of higher order.

6. Combined invariants

One of the main benefits of the assumption that the covariance matrix is not constrained to be diagonal is the existence of *combined invariants* to blur and affine transformation of the coordinates. If the blurring Gaussian kernel was assumed in the axial position and hence C was constrained to be diagonal, we could never combine blur with an affine transformation or rotation, because it would violate the assumption. This is why the combined invariants have not been constructed yet (except a very special case of a unitary covariance matrix and rotation, see [22]).

The key idea of designing the combined invariants follows from the observation how the primordial image is transformed if the original image has undergone an affine transformation $f'(\mathbf{x}) = f(A\mathbf{x})$. By means of Propositions 3–5, it is easy to show that

$$I(f')(\mathbf{u}) = I(f)(A^{-T}\mathbf{u}).$$

Applying inverse Fourier transform, we get

$$f_r'(\mathbf{x}) = \|A\| f_r(A\mathbf{x}),$$

where f_r' is the primordial image of f'. This relation tells us that the primordial image is transformed by *the same* coordinate transformation as the original image.

Since the invariants M_{pq} in Eq. (15) are in a fact moments of f_r, we can simply substitute them into any affine or rotation moment invariant (we only should avoid those containing second-order moments because they would lead to trivial invariants) and we end up

with the combined invariant. The theory of both affine and rotation moment invariants has been well elaborated and several complete and independent invariant sets are available, see for instance [1,27–31]. Since blur invariants M_{pq} also form a complete and independent set (see Theorem 2), we get in this way a complete and independent set of combined invariants. This strong result is summarized in the following Theorem.

Theorem 3 (Substitution Theorem). *Let f be an image function and let M_{pq} be invariants w.r.t. Gaussian blur defined by Eq. (15). Let $f'(\mathbf{x}) = f(A\mathbf{x})$, A being a regular 2 × 2 matrix. Let $J(m_{pq}|p, q = 0, \ldots, r)$ be an absolute invariant of image moments w.r.t. A, i.e. $J(m'_{pq}|p, q = 0, \ldots, r) = J(m_{pq}|p, q = 0, \ldots, r)$. Then $J(M_{pq}|p, q = 0, \ldots, r)$ is a relative invariant w.r.t. both A and Gaussian blur as*

$$\|A\|^w J(M'_{pq}| p, q = 0, \ldots, r) = J(M_{pq}|p, q = 0, \ldots, r),$$

where w is the weight[3] of invariant $J(m_{pq}|p, q = 0, \ldots, r)$.

Proof. Since $f'_r(\mathbf{x}) = \|A\| f_r(A\mathbf{x})$, the moments M'_{pq} of $f'_r(\mathbf{x})$ are related to the moments $\tilde{M}_{pq}$ of $f_r(A\mathbf{x})$ as $M'_{pq} = \|A\|\tilde{M}_{pq}$ for any p and q. In the theory of affine moment invariants [1,29], it is well known that any absolute invariant $J(m_{pq}| p, q = 0, \ldots, r)$ must have a form of a finite sum, where all terms are products of K moments (K is called the *degree* of the invariant) divided by $(K + w)$-th power of m_{00}. The statement of Theorem 3 follows immediately from this fact. Note that the invariance of $J(M_{pq}| p, q = 0, \ldots, r)$ w.r.t. Gaussian blur is obvious and does not depend on the order in which the blurring and the coordinate transformation A have been applied. They are commutative in the sense that $(f * h)' = 1/\|A\|(f' * h')$ and still $h' \in S$ thanks to Proposition 5. $\square$

Since A is usually unknown in practice, absolute invariants are more convenient image descriptors than the relative ones. An absolute combined invariant can be obtained as a ratio of two relative invariants of the same weight or, more generally, as a ratio of any two products of various relative invariants such that the factor $\|A\|$ is cancelled.

7. Experiments

Numerical experiments presented in this section aim to illustrate the properties of the proposed invariants, namely to evaluate the invariance w.r.t. arbitrary Gaussian blur, the recognition power and the robustness to additive noise. First, we prove the invariance on static images and also on a real video, where the Gaussian blur model is not exactly valid. As sample applications, we show how the blur invariants can be used for object tracking in a video and for recognition of blurred faces. A comparison to other state-of-the-art methods is given. Finally, we show the performance of the combined affine-blur invariants in digit recognition.

7.1. Invariance verification on public datasets

This basic experiment is a verification of the invariance of functionals M_{pq} from Eq. (15). We used two public-domain image databases, which contain series of Gaussian-blurred images (see Fig. 6 for two examples). We used 30 series (original and five blurred instances of various extent of the blur) from the CID:IQ dataset [32] and 23 series from the CSIQ dataset [33]. For each of them, we calculated the invariants up to the 9th order. The relative error of all invariants on each image series was always between 10^{-4} and 10^{-3}, which illustrates a perfect invariance. The fluctuation within a single series is so small that in no way diminishes

---

[3] The term *weight of an invariant* has been commonly used in the theory of algebraic invariants, see for instance [1], [29] for the definition. For any given invariant, its weight is known and follows from the way how the invariant has been constructed.

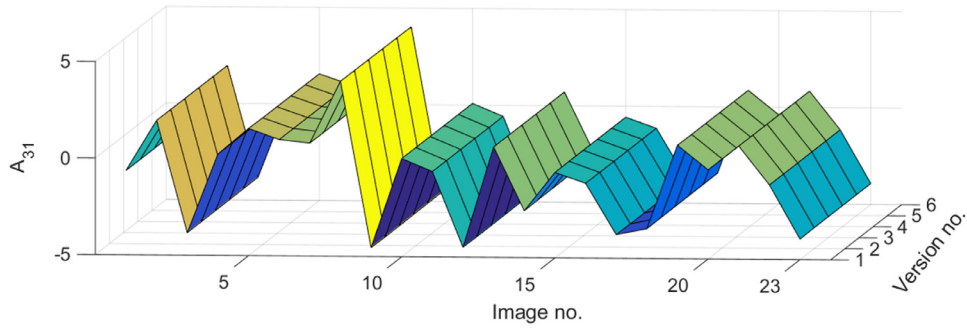**Fig. 6.** Two examples of the Gaussian-blurred image series from the CSIQ database.

Fig. 7. The values of a single invariant calculated over 23 series (from left to right) consisting of six blurred instances of the originals (from front to back). The value is always almost constant within each individual series while significantly different for distinct images.
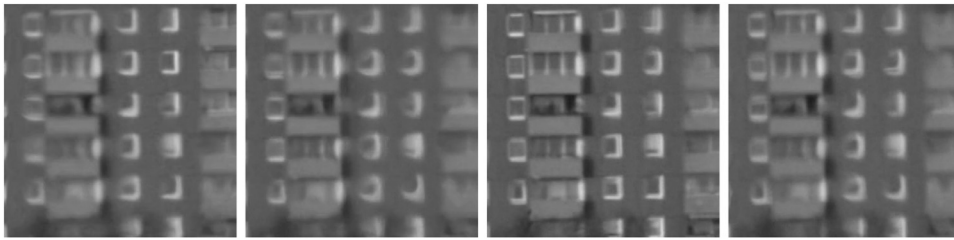

Fig. 8. Four sample frames of a video blurred due to the hot air turbulence.

the ability to discriminate two different originals, as is illustrated in Fig. 7.

7.2. Verification on a real video

In this experiment, we used publicly accessible video[4] from [7] showing a static scene (front side of a building) captured intentionally through a turbulent hot air. Due to the turbulence, the video is degraded by a time-varying blur, which is, according to [7], expected to be approximately Gaussian. Four sample frames of the sequence are shown in Fig. 8.

Similarly to the previous experiment, we calculated the blur invariants M_{pq} from Eq. (15) up to the 8th order for each frame. The graph in Fig. 9 summarizes the results. It is worth noting that the invariants exhibit a perfect stability even if the real blur is probably not exactly Gaussian.

7.3. Tracking in a video

The proposed blur invariants can be used also for tracking objects in a blurred video. We took an indoor video that starts with a clear frame. Then the video becomes more and more blurred. The blur is Gaussian with a time-varying covariance matrix. In the first frame, we chose the template of interest that we track by invariant template matching in the rest of the video.
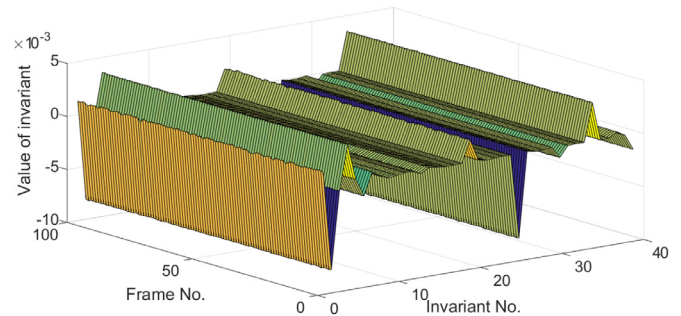

Fig. 9. The values of the invariants up to the 8th order calculated over 99 frames of a video corrupted by a real turbulence blur. The value of each invariant is always almost constant on all frames.

To show the strength of the method, each frame was processed independently (in reality, the motion information could be used to speed up and stabilize the tracking but here we wanted to demonstrate solely the performance of the invariants). We can evaluate visually that the tracking is reasonably stable and accurate and actually follows the real motion of the template. Sample frames with the detected template are shown in Fig. 10.[5]

---

[4] http://alumni.soe.ucsc.edu/~xzhu/doc/turbulence.html.

[5] The full video is available at http://zoi.utia.cas.cz/files/Tracking_changing_blur_5th_order.gif.

Fig. 10. Tracking in a blurred video. The initial clear image with the template (top left), sample frames of the blurred video with the template detected.

Table 1
The recognition rate [%] of the tested methods for Gaussian blur of various size.

Blur size (Gaussian)	Invariants	Zhang	Lébl	Gopalan
7 × 7	100	100	100	74
11 × 11	100	86	100	25
15 × 15	100	48	100	5

7.4. Recognition of blurred faces

In this experiment we show the performance of the proposed invariants in face recognition applied on blurred photographs. We compare the proposed method with the blur-invariant distances proposed by Gopalan et al. [13], Zhang et al. [11], and Lébl et al. [15] (see Section 2.3 for a brief description of these competitors). We calculated also the standard ℓ_2-distance, which does not take the blur into account at all, but it expectedly failed completely so we did not include it in the tables.

We used 38 distinct human faces from the Extended Yale Face Database B [34] (the same database was used in [13]). This database contains clear faces only, so we created the blurred and noisy query images artificially (see Fig. 11 for some examples). In all tests, moment invariants up to the 9th order were used.

First, we tested the recognition rate as a function of the blur size. The blurred, noise-free query image was always classified against the clear 38-image database. While moment invariants and the Lébl's method are 100% successful even for relatively large blurs, the Gopalan's method surprisingly does not reach comparable results. Its success rate drops very rapidly with the increasing blur size, even if we provided the correct blur size as the input parameter of the algorithm. The Zhang's method performs well for small blurs (see Table 1). It should be pointed out, that the reported 100% success rate of the invariants was achieved thanks to a controlled noise-free environment, where the Gaussian convolution model held perfectly. In the next two experiments, these ideal conditions will be relaxed and we will monitor the impact on the method performance.

If we apply a significantly non-Gaussian blur (we used a directional motion blur in this experiment), we observe a drop of the performance of the invariants, while the other methods perform more or less the same as in the case of Gaussian blur (see Table 2). This is not surprising, because the derivation of the invariants was inherently based on the assumption of a Gaussian blur while the Gopalan's and Lébl's methods assume only the knowledge of the blur size, which was fulfilled in this experiment. The invariants are relatively sensitive to the violation of the Gaussian blur shape.

Then, we tested the noise robustness of all methods. We corrupted the query images with an additive white normally dis-

Table 2
The recognition rate [%] of the tested methods for a motion blur of various size.

Blur size (motion)	Invariants	Zhang	Lébl	Gopalan
7 × 7	87	100	100	99
11 × 11	71	72	100	76
15 × 15	45	17	100	40

Table 3
Noise robustness test: The recognition rate [%] achieved for various SNR.

SNR [dB]	Invariants	Zhang	Lébl	Gopalan	OG Invariants
20	100	100	100	76	100
10	100	55	100	51	100
5	99	44	99	37	99
2	97	37	87	27	97
0	92	32	79	26	95

tributed noise of SNR from 20 dB to 0 dB. The success rate of the invariants as well as of the Lébl's method remains very high even for heavy noise, while the other two methods appear to be vulnerable. Table 3 summarizes the results. High robustness of the invariants can be explained by the fact that the moments, being integral features, average-out the noise.

Many papers on moments have shown experimentally that orthogonal (OG) moments are more robust to numerical errors and also to noise. This is due to the fact that OG moments can be calculated indirectly using recurrent formulas, which avoids working with very high and very low numbers. For this reason, various OG moments have been implemented in moment invariants, where they replace traditional geometric moments (see [1], Chapter 7, for a survey of OG moments). In the context of blur invariants (but not to Gaussian blur), this approach was applied for instance in [35–41].[6] We tested the use of Legendre moments in the proposed Gaussian blur invariants. We expressed geometric moments as functions of Legendre moments, substituted these functions into (15) and obtained in this way blur invariants in terms of Legendre moments. We applied these invariants on the same noisy facial images as above. The results are shown in the rightmost column of Table 3. The recognition rate is the same as for the invariants from geometric moments except SNR = 0 dB, where a slightly better robustness of OG moments appears.

Finally, we compared the speed of all methods. We evaluated it as a function of the image size. The results are shown in Fig. 12. The time refers to a single query and does not comprise any pre-calculations on the database images.

The proposed invariants work with a highly-compressed image representation (only the moments up to the 9th order were used). All other methods use a complete pixel-wise representation, however with various time-efficiency. The Lébl's method is the most efficient for small images. As the image size increases, moment invariants become more time efficient. They outperform the Lébl's method for images larger than approximately 600 × 600 pixels. It should be noted, that the complexity of calculation of the invariants is determined solely by the complexity of moment computation. For a graylevel $N \times N$ image, this is typically $O(N^2)$ and does not depend on the actual blur size (unlike the Zhang's and Gopalan's methods). Although some faster algorithms exist for moment computation [43], we did not use them here because they are efficient for special types of images only.

---

[6] It should be noted that the use of OG moments in blur invariants is solely because of their favorable numerical properties. As proved by Kautsky [42], blur invariants in any two distinct polynomial bases are theoretically equivalent.
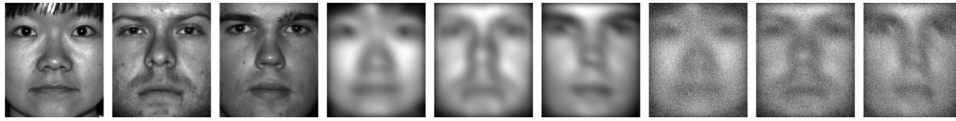
Fig. 11. Sample face images used in the experiments: clear database faces (images 1–3), blurred (images 4–6) and noisy (images 7–9) query images.
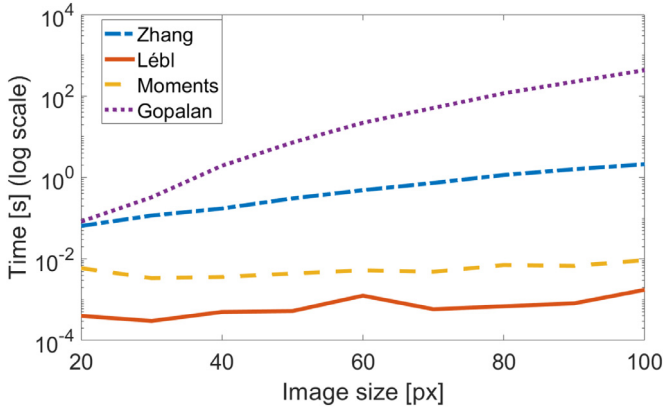

Fig. 12. Time [s] needed to compare a query image to a single database image as a function of the image size. The blur size was fixed at 15 × 15 pixels. The time axis is shown in a logarithmic scale.
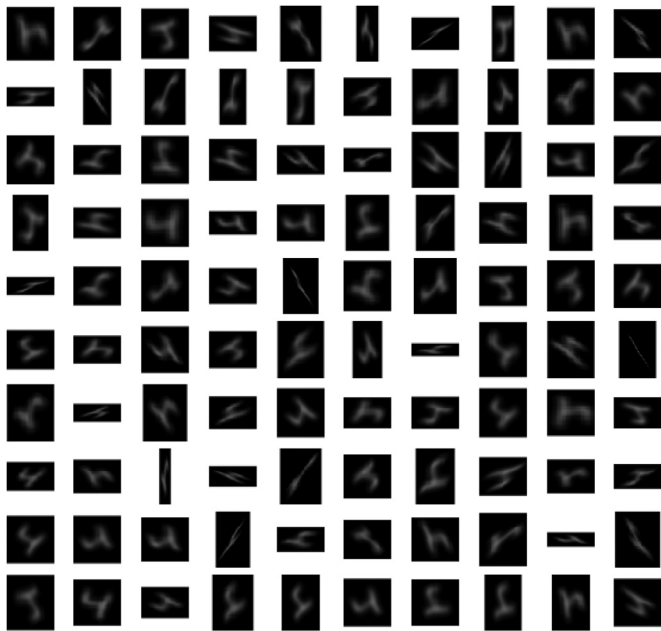

Fig. 13. 100 randomly blurred and affinely deformed pictures of digit 4.

7.5. Recognition of blurred and affinely deformed objects

In the last experiment, we demonstrate the power of the combined affine-blur invariants proposed in Section 6. For this test, we used the popular MNIST dataset of handwritten digits [44]. For each digit $0, 1, \ldots, 9$ we randomly generated 100 blurred and affinely deformed samples (see Fig. 13 showing the test set of the digit 4) and classified them against the original dataset. The affine-blur invariants used in this test were constructed according to the Substitution Theorem (Theorem 3), where we used the well-established Affine moment invariants (AMIs) [29] as $J(m_{pq})$.

To illustrate the advantage of the combined invariants, we compared them both to "pure" AMIs [29] and to "pure" Gaussian blur invariants (15). The combined invariants yielded the overall recognition rate 98.5 %, while the AMIs only 20 % and the blur invariants performed even worse yielding 15.6 % success rate. This clearly

shows that the Substitution Theorem brings invariants of a new quality.

The comparison to the Gopalan's, Zhang's, and Lébl's invariant distances as in the face recognition experiment does not make sense here because all those methods require the images to be precisely geometrically aligned and collapse completely in case of spatial misalignment.

8. Conclusion

Blur invariants w.r.t. blur kernels which are defined by certain generic properties rather than by their parametric form were already discovered for centrosymmetric [17], radial [45], N-fold rotational symmetric [18,46], and N-fold dihedral [47] blurs, respectively. In this paper, we focused on parametric kernels since they allow to derive more specific invariants which yields a better discrimination power. We proposed new invariants w.r.t. Gaussian blur. Unlike all earlier works on Gaussian blur, our method does not require the Gaussian blurring kernel to be circularly symmetric and works with arbitrary Gaussians. We found a non-linear projection operator by means of which the invariants are defined in the Fourier domain. Equivalently, the invariants can be calculated directly in the image domain, without an explicit construction of the projections. We showed that the new invariants can be made invariant also to a linear transformation of the coordinates thanks to the Substitution Theorem, which was not possible in case of earlier Gaussian-blur invariants. Experimental evaluation and comparison to alternative approaches (namely to various blur-invariant distances) showed a superior performance in most scenarios in terms of the recognition rate and speed.

In a future work, it would be interesting to couple the proposed blur-invariant representation with the CNNs in order to make the CNNs blur-invariant without any data augmentation. CNNs probably cannot be fed directly with the moment invariant (15). Instead, we envisage to use the Fourier-domain invariants (8) for this purpose. However, since the distinctive patterns in spectral domain are totally different from those in the image domain, one probably cannot use any publicly available pre-trained network and will have to train (and maybe also to design) the network by himself.

Declaration of Competing Interest

None.

Acknowledgments

References

[1] J. Flusser, T. Suk, B. Zitová, 2D and 3D Image Analysis by Moments, Wiley, Chichester, U.K., 2016.

[2] B. Honarvar, R. Paramesran, C.-L. Lim, Image reconstruction from a complete set of geometric and complex moments, Signal Processing 98 (2014) 224–232.

[3] A.S. Carasso, The APEX method in image sharpening and the use of low exponent Lévy stable laws, SIAM J. Appl. Math. 63 (2) (2003) 593–618.

[4] J.H. Elder, S.W. Zucker, Local scale control for edge detection and blur estimation, IEEE Trans Pattern Anal Mach Intell 20 (7) (1998) 699–716.

[5] W. Zhang, W.-K. Cham, Single-image refocusing and defocusing, IEEE Trans. Image Process. 21 (2) (2012) 873–882.

[6] F. Xue, T. Blu, A novel SURE-based criterion for parametric PSF estimation, IEEE Trans. Image Process. 24 (2) (2015) 595–607.

[7] X. Zhu, P. Milanfar, Removing atmospheric turbulence via space-invariant deconvolution, IEEE Trans. Pattern Anal. Mach. Intell. 35 (1) (2013) 157–170.

[8] P. Campisi, K. Egiazarian, Blind Image Deconvolution: Theory and Applications, CRC, 2007.

[9] L. Taylor, G. Nitschke, Improving deep learning using generic data augmentation, arXiv preprint arXiv:1708.06020 (2017).

[10] Y. Pei, Y. Huang, Q. Zou, X. Zhang, S. Wang, Effects of image degradation and degradation removal to CNN-based image classification, IEEE Trans. Pattern Anal. Mach. Intell. (2019), doi:10.1109/TPAMI.2019.2950923.

[11] Z. Zhang, E. Klassen, A. Srivastava, P. Turaga, R. Chellappa, Blurring-invariant Riemannian metrics for comparing signals and images, in: IEEE International Conference on Computer Vision, ICCV'11, 2011, pp. 1770–1775.

[12] Z. Zhang, E. Klassen, A. Srivastava, Gaussian blurring-invariant comparison of signals and images, IEEE Trans. Image Process. 22 (8) (2013) 3145–3157.

[13] R. Gopalan, P. Turaga, R. Chellappa, A blur-robust descriptor with applications to face recognition, IEEE Trans. Pattern Anal. Mach. Intell. 34 (6) (2012) 1220–1226.

[14] P. Vageeswaran, K. Mitra, R. Chellappa, Blur and illumination robust face recognition via set-theoretic characterization, IEEE Trans. Image Process. 22 (4) (2013) 1362–1372.

[15] M. Lébl, F. Šroubek, J. Kautský, J. Flusser, Blur invariant template matching using projection onto convex sets, in: Proc. 18th Int'l. Conf. Computer Analysis of Images and Patterns CAIP'19, 2019, pp. 351–362.

[16] J. Flusser, T. Suk, S. Saic, Recognition of blurred images by the method of moments, IEEE Trans. Image Process. 5 (3) (1996) 533–538.

[17] J. Flusser, T. Suk, Degraded image analysis: an invariant approach, IEEE Trans. Pattern Anal. Mach. Intell. 20 (6) (1998) 590–603.

[18] J. Flusser, T. Suk, J. Boldyš, B. Zitová, Projection operators and moment invariants to image blurring, IEEE Trans. Pattern Anal. Mach. Intell. 37 (4) (2015) 786–802.

[19] J. Liu, T. Zhang, Recognition of the blurred image by complex moment invariants, Pattern Recognit. Lett. 26 (8) (2005) 1128–1138.

[20] B. Xiao, J.-F. Ma, J.-T. Cui, Combined blur, translation, scale and rotation invariant image recognition by Radon and pseudo-Fourier-Mellin transforms, Pattern Recognit. 45 (2012) 314–321.

[21] C. Höschl IV, J. Flusser, Robust histogram-based image retrieval, Pattern Recognit. Lett. 69 (1) (2016) 72–81.

[22] J. Flusser, S. Farokhi, C. Höschl IV, T. Suk, B. Zitová, M. Pedone, Recognition of images degraded by Gaussian blur, IEEE Trans. Image Process. 25 (2) (2016) 790–806.

[23] V. Ojansivu, J. Heikkilä, Blur insensitive texture classification using local phase quantization, in: A. Elmoataz, O. Lezoray, F. Nouboud, D. Mammass (Eds.), Image and Signal Processing ICISP'08, Lecture Notes in Computer Science, 5099, Springer, Berlin, Heidelberg, Germany, 2008, pp. 236–243.

[24] J. Kostková, J. Flusser, M. Lébl, M. Pedone, Image invariants to anisotropic Gaussian blur, in: Proceedings of the Scandinavian Conf. Image Analysis SCIA'19, LNCS 11482, Springer, 2019, pp. 140â–151.

[25] L. Isserlis, On a formula for the product-moment coefficient of any order of a normal frequency distribution in any number of variables, Biometrika 12 (1/2) (1918) 134–139.

[26] D. von Rosen, Moments for matrix normal variables, Statistics: J. Theoret. Appl.Stat. 19 (4) (1988) 575–583.

[27] J. Flusser, On the independence of rotation moment invariants, Pattern Recognit. 33 (9) (2000) 1405–1410.

[28] T.H. Reiss, The revised fundamental theorem of moment invariants, IEEE Trans. Pattern Anal. Mach. Intell. 13 (8) (1991) 830–834.

[29] T. Suk, J. Flusser, Affine moment invariants generated by graph method, Pattern Recognit. 44 (9) (2011) 2047–2056.

[30] B. Xiao, J.-T. Cui, H.-X. Qin, W.-S. Li, G.-Y. Wang, Moments and moment invariants in the Radon space, Pattern Recognit. 48 (9) (2015) 2772–2784.

[31] B. Xiao, L. Li, Y. Li, W. Li, G. Wang, Image analysis by fractional-order orthogonal moments, Inf. Sci. 382 (2017) 135–149.

[32] X. Liu, M. Pedersen, J.Y. Hardeberg, CID: IQ–a new image quality database, in: International Conference on Image and Signal Processing, Springer, 2014, pp. 193–202.

[33] E.C. Larson, D.M. Chandler, Most apparent distortion: full-reference image quality assessment and the role of strategy, J. Electron Imaging 19 (1) (2010) 11006.

[34] A.S. Georghiades, P.N. Belhumeur, D.J. Kriegman, From few to many: illumination cone models for face recognition under variable lighting and pose, IEEE Trans. Pattern Anal. Mach. Intell. 23 (6) (2001) 643–660.

[35] H. Zhang, H. Shu, G.-N. Han, G. Coatrieux, L. Luo, J.L. Coatrieux, Blurred image recognition by Legendre moment invariants, IEEE Trans. Image Process. 19 (3) (2010) 596–611.

[36] C.-Y. Wee, R. Paramesran, Derivation of blur-invariant features using orthogonal Legendre moments, IET Comput. Vision 1 (2) (2007) 66–77.

[37] H. Zhu, M. Liu, H. Ji, Y. Li, Combined invariants to blur and rotation using Zernike moment descriptors, Pattern Anal. Appl. 3 (13) (2010) 309–319.

[38] B. Chen, H. Shu, H. Zhang, G. Coatrieux, L. Luo, J.L. Coatrieux, Combined invariants to similarity transformation and to blur using orthogonal Zernike moments, IEEE Trans. Image Process. 20 (2) (2011) 345–360.

[39] H. Ji, H. Zhu, Degraded image analysis using Zernike moment invariants, in: Proceedings of the International Conference on Acoustics, Speech and Signal Processing ICASSP'09, 2009, pp. 1941–1944.

[40] X. Dai, T. Liu, H. Shu, L. Luo, Pseudo-Zernike moment invariants to blur degradation and their use in image recognition, in: J. Yang, F. Fang, C. Sun (Eds.), Intelligent Science and Intelligent Data Engineering IScIDE'12, Lecture Notes in Computer Science, 7751, Springer, 2013, pp. 90–97.

[41] Q. Liu, H. Zhu, Q. Li, Image recognition by combined affine and blur Tchebichef moment invariants, in: Proceedings of 4th International Conference on Image and Signal Processing (CISP), 2011, pp. 1517–1521.

[42] J. Kautsky, J. Flusser, Blur invariants constructed from arbitrary moments, IEEE Trans. Image Process. 20 (12) (2011) 3606–3611.

[43] T. Suk, C. Höschl IV, J. Flusser, Decomposition of binary images – a survey and comparison, Pattern Recognit. 45 (12) (2012) 4279–4291.

[44] Y. LeCun, C. Cortes, MNIST handwritten digit database, 2010, http://yann.lecun.com/exdb/mnist/.

[45] J. Flusser, B. Zitová, Invariants to convolution with circularly symmetric PSF, in: Proceedings of the 17th International Conference on Pattern Recognition ICPR'04, IEEE Computer Society, 2004, pp. 11–14.

[46] M. Pedone, J. Flusser, J. Heikkilä, Blur invariant translational image registration for N-fold symmetric blurs, IEEE Trans. Image Process. 22 (9) (2013) 3676–3689.

[47] M. Pedone, J. Flusser, J. Heikkilä, Registration of images with N-fold dihedral blur, IEEE Trans. Image Process. 24 (3) (2015) 1036–1045.

Jitka Kostková received the M.Sc. degree in Applied Mathematical Stochastic Methods from the Czech Technical University, Faculty of Nuclear Science and Physical Engineering, Prague, Czech Republic, in 2015. Currently, she is a Ph.D. student in Mathematical Engineering and tutors undergraduate courses on mathematical analysis at the same university. Jitka Kostková's research interest is focused on moments and moment invariants.

Jan Flusser received the M.Sc. degree in mathematical engineering from the Czech Technical University, Prague, Czech Republic, in 1985, the Ph.D. degree in computer science from the Czechoslovak Academy of Sciences in 1990, and the DrSc. degree in technical cybernetics in 2001. Since 1985 he has been with the Institute of Information Theory and Automation, Czech Academy of Sciences, Prague. In 1995–2007, he was holding the position of a head of Department of Image Processing. Since 2007 he has been a Director of the Institute. He is a full professor of computer science at the Czech Technical University, Faculty of Nuclear Science and Physical Engineering, and at the Charles University, Faculty of Mathematics and Physics, Prague, Czech Republic, where he gives undergraduate and graduate courses on Digital Image Processing, Pattern Recognition, and Moment Invariants and Wavelets. Jan Flusser's research interest covers moments and moment invariants, image registration, image fusion, multichannel blind deconvolution, and superresolution imaging. He has authored and coauthored more than 200 research publications in these areas, including the monographs *Moments and Moment Invariants in Pattern Recognition* (Wiley, 2009) and *2D and 3D Image Analysis by Moments* (Wiley, 2016). In 2007 Jan Flusser received the Award of the Chairman of the Czech Science Foundation for the best research project and won the Prize of the Academy of Sciences of the Czech Republic for the contribution to image fusion theory. In 2010, he was awarded by the SCOPUS 1000 Award. He received the Felber Medal of the Czech Technical University for excellent contribution to research and education in 2015 and the Academic Premium of the Czech Academy of Sciences for outstanding researchers in 2017.

Matteo Pedone received the M.Sc. degree in computer science from "La Sapienza" University of Rome, Italy, in 2007, and the Doctor of Technology (Ph.D.) degree in computer science from the University of Oulu, Finland, in 2015. He is currently a post-doctoral researcher at the Center for Machine Vision Research, University of Oulu, Finland. His research interests include computer vision, computational photography, invariant theory, statistical signal processing, differential geometry, and Clifford algebra.

Matěj Lébl received the M.Sc. degree in Numerical and Computational Mathematics from the Charles University, Faculty of Mathematics and Physics, Prague, Czech Republic, in 2017. Currently, he is a Ph.D. student in Informatics.